Supplementary Material

Redox isomerization of allylic alcohols catalyzed by new water-soluble Rh(I)-N-heterocyclic carbene complexes

Csilla Enikő Czégéni[a]*, Marianna Fekete[b], Eszter Tóbiás[b], Antal Udvardy[b], Henrietta Horváth[a], Gábor Papp[b], Ferenc Joó[a,b]

[a]MTA-DE Redox and Homogeneous Catalytic Reaction Mechanisms Research Group, P.O.Box 400, Debrecen, H-4002 Hungary

[b]University of Debrecen, Department of Physical Chemistry, P.O.Box 400, Debrecen, H-4002 Hungary

*Corresponding author:

E-mail: nagy.csilla@science.unideb.hu

Contents

Gas chromatographic analysis of the reaction mixtures

Gas chromatographic measurements were done with an Agilent Technologies 7890 A instrument (HP-5, 0.25µm x 30 m x 0.32 mm, FID 300 °C (Agilent Technologies, Santa Clara, California, USA); carrier gas: nitrogen 1.9 mL/min). T_{inj}= 250 °C, T_{det}= 300°C, V_{inj}= 1 µL, split ratio = 350:1. The temperature of the column was 90 °C. Usually the reaction mixtures were extracted at room temperature with chloroform (2 mL) and the organic layer was dried on $MgSO_4$.

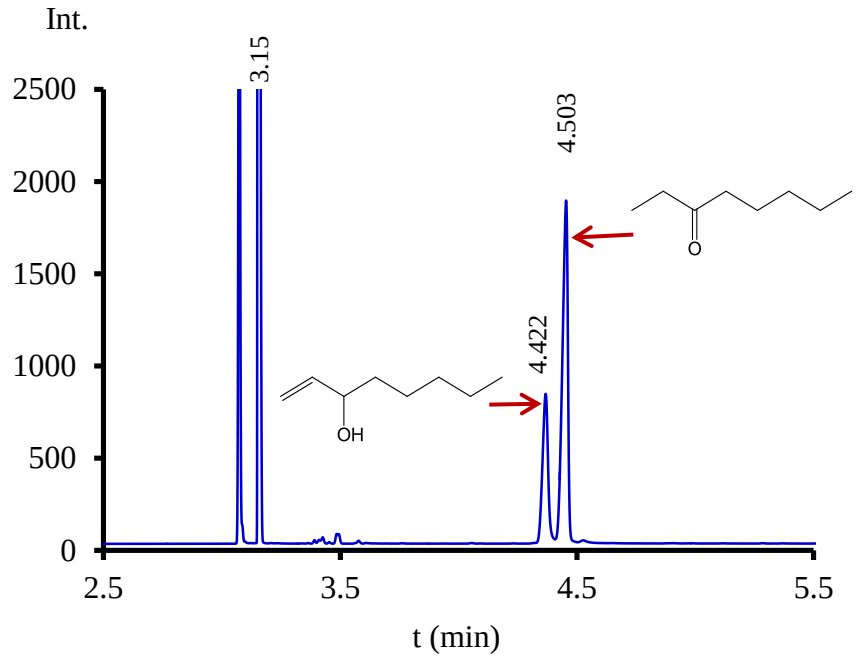

Figure S1. Gas chromatographic separation of the substrate (oct-1-en-3-ol) and product (oct-1-en-3-on) of redox isomerization of oct-1-en-3-ol.

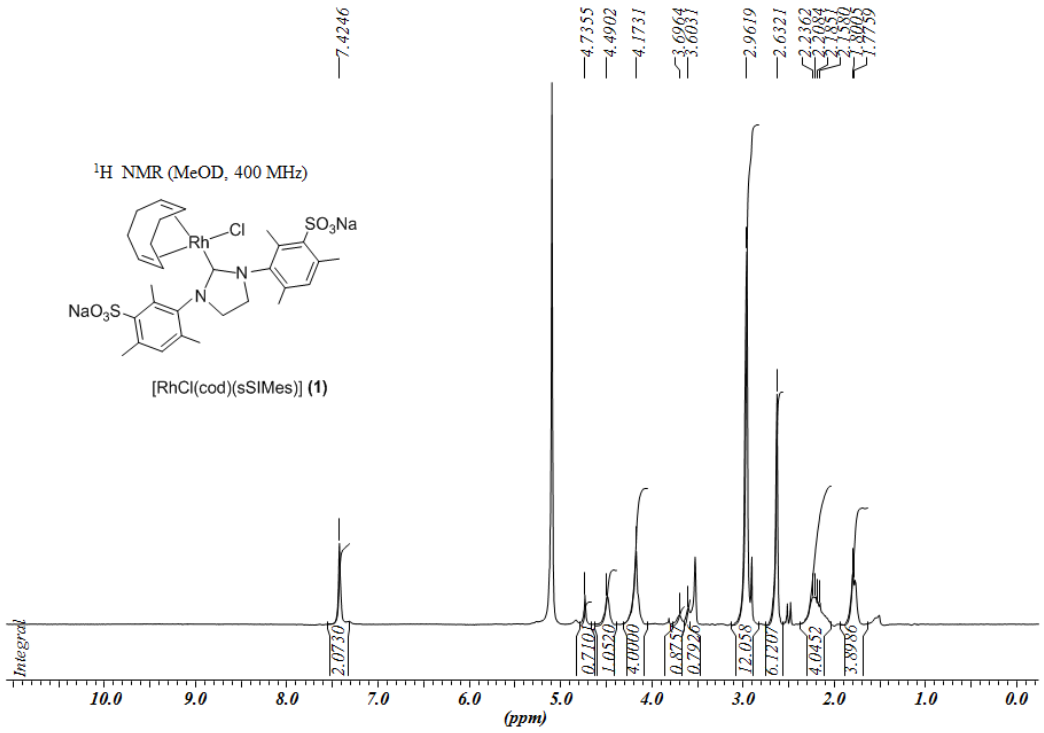

Figure S2. ^{1}H-NMR spectrum of [RhCl(cod)(sSIMes)] (**1**)

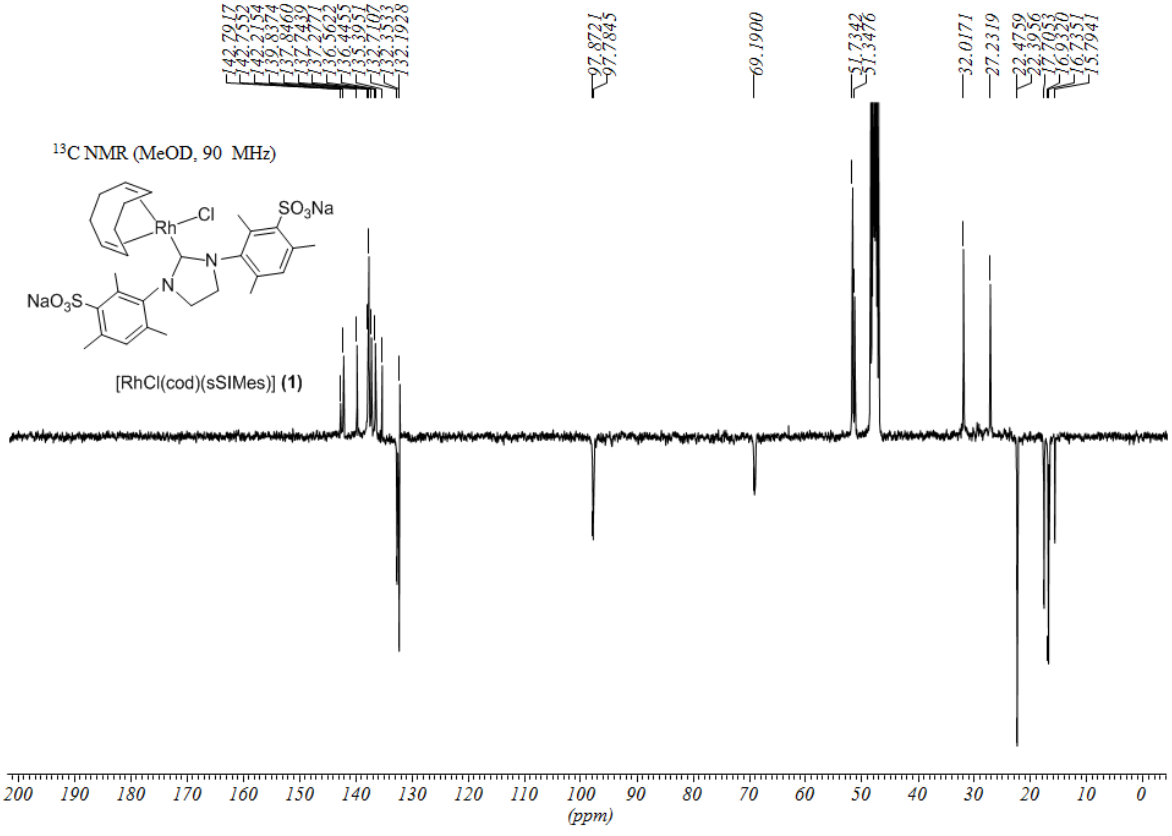

Figure S3. ^{13}C{^{1}H} NMR spectrum of [RhCl(cod)(sSIMes)] (**1**)

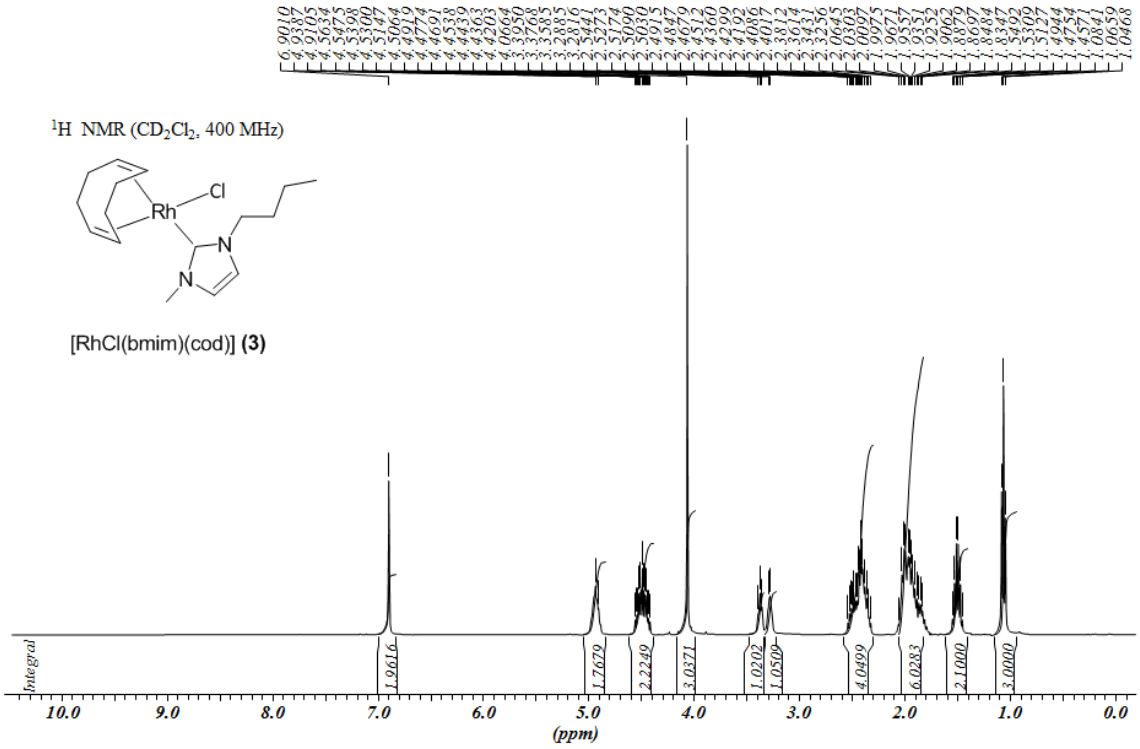

Figure S4. ^{1}H-NMR spectrum of [RhCl(bmim)(cod)] (**3**).

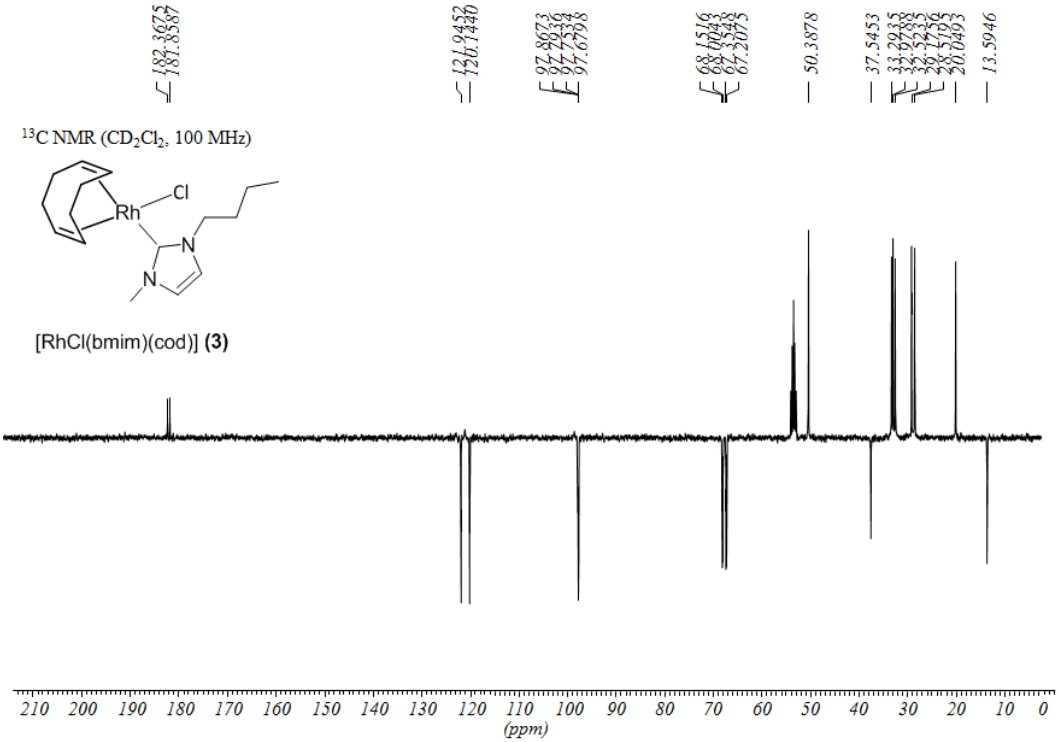

Figure S5. ^{13}C{^{1}H} NMR spectrum of [RhCl(bmim)(cod)] (**3**).

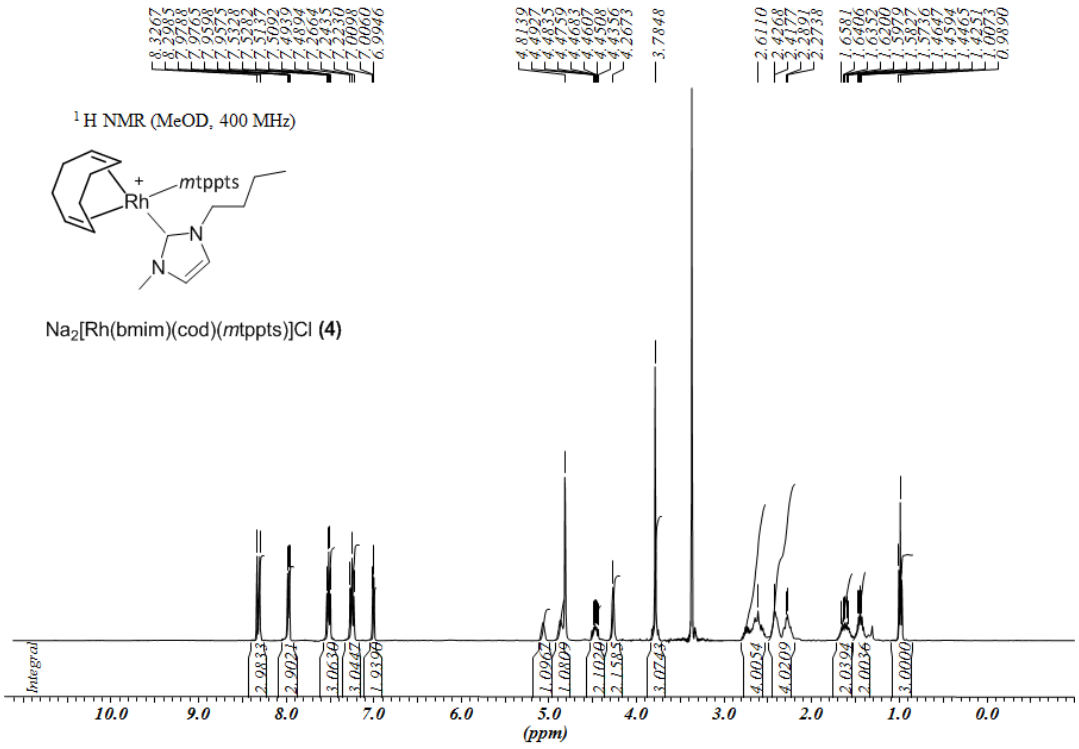

Figure S6. ^{1}H-NMR spectrum of Na_2[Rh(bmim)(cod)(*m*tppts)] (**4**).

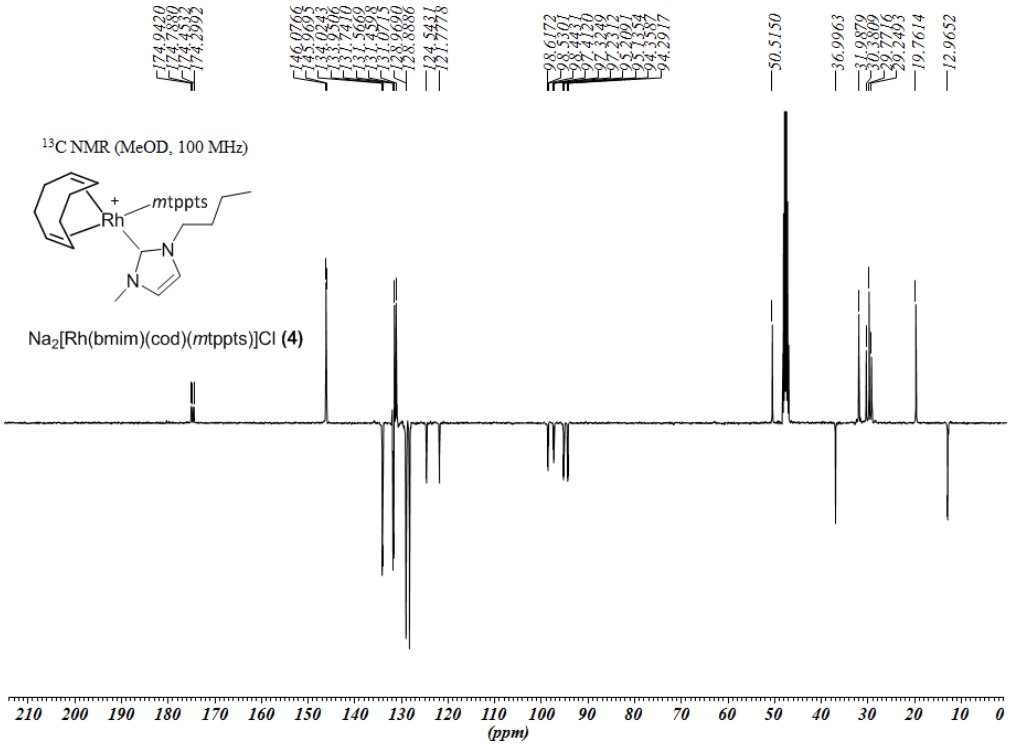

Figure S7. ^{13}C{^{1}H} NMR spectrum of Na_2[Rh(bmim)(cod)(*m*tppts)](**4**).

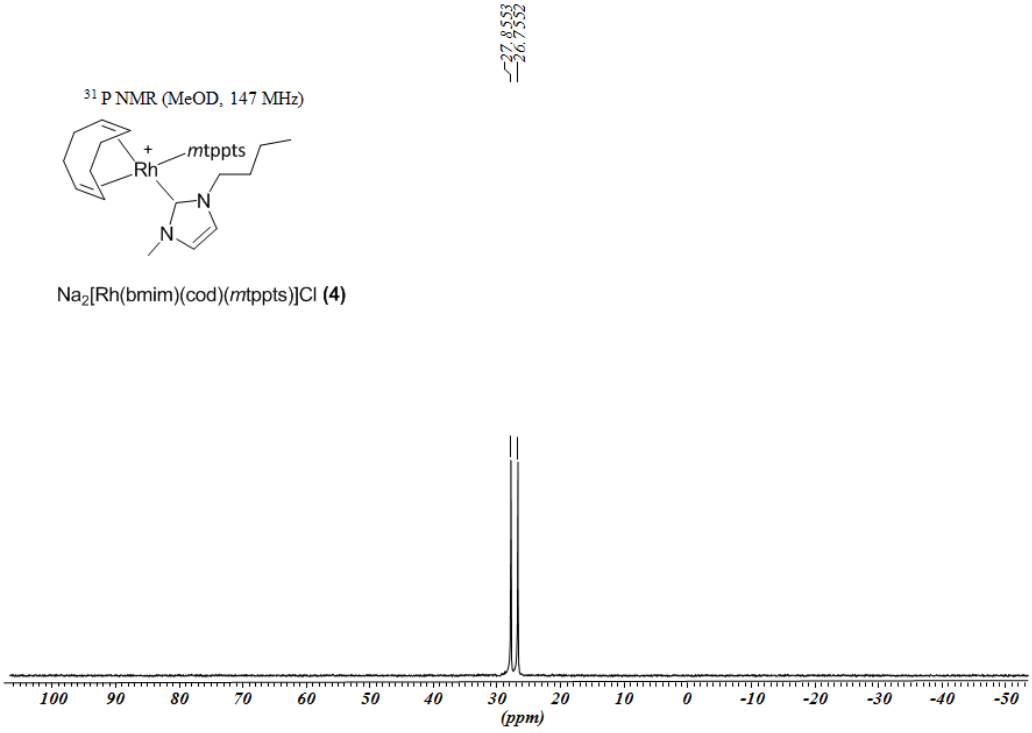

Figure S8. $^{31}P\{^{1}H\}$ NMR spectrum of Na_2[Rh(bmim)(cod)(*m*tppts)](**4**).

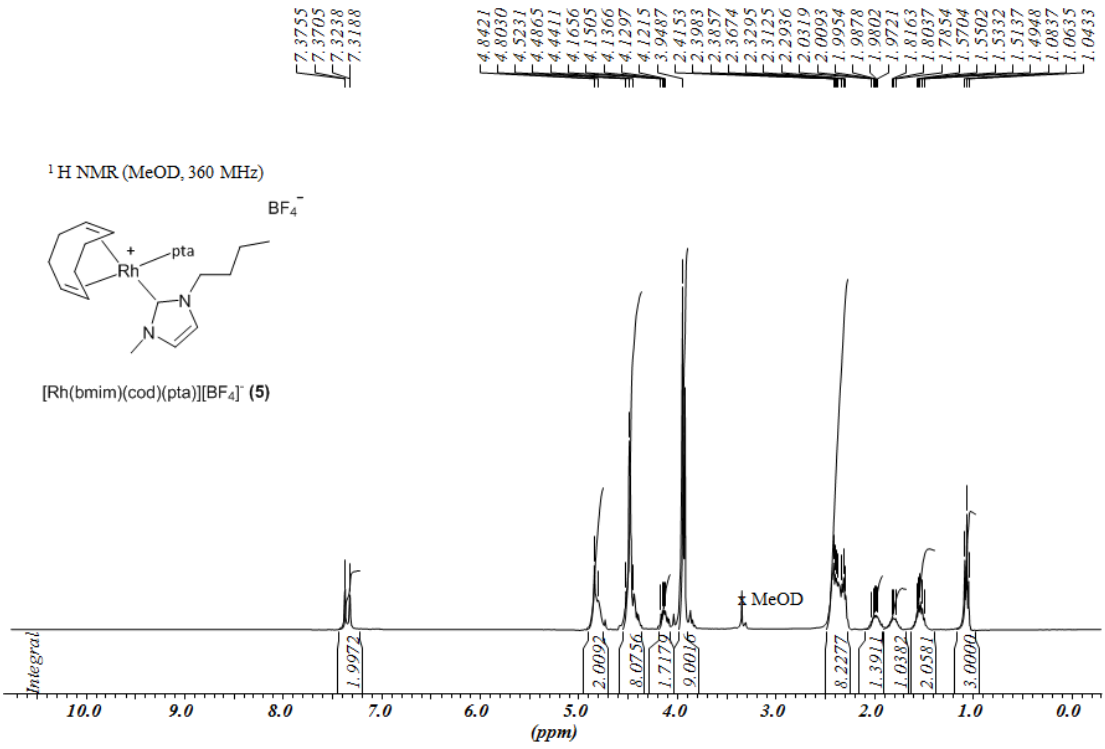

Figure S9. ^{1}H-NMR spectrum of [Rh(bmim)(cod)(pta)]BF_4 (**5**).

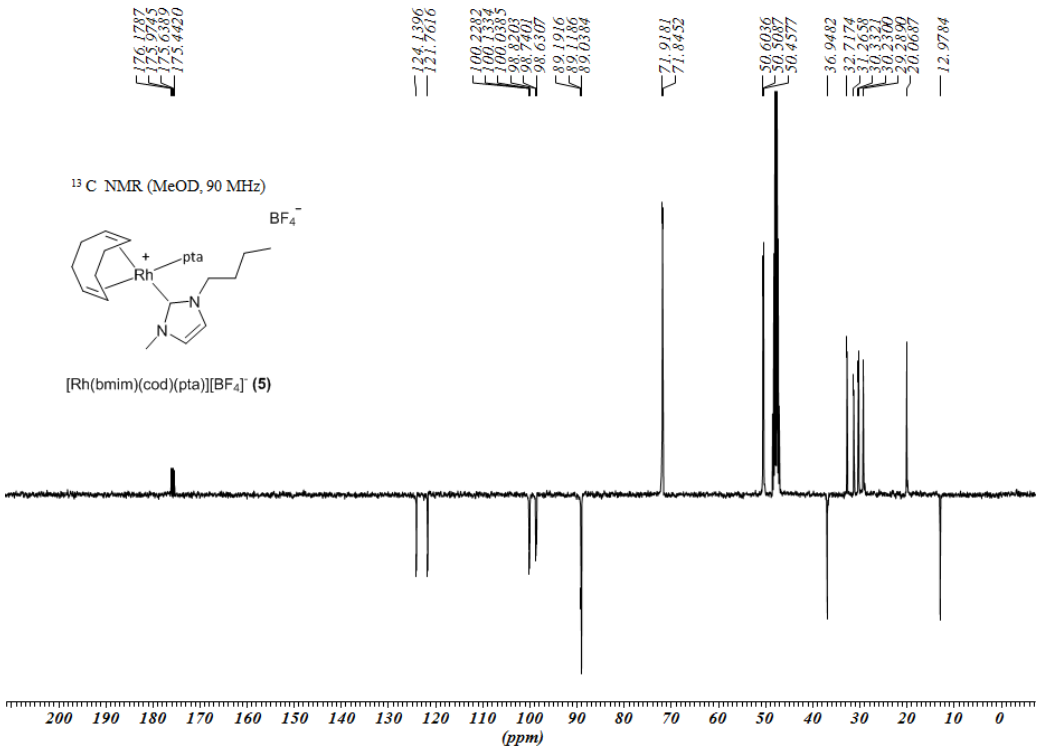

Figure S10. ^{13}C{^{1}H} NMR spectrum of [Rh(bmim)(cod)(pta)]BF_4 (**5**).

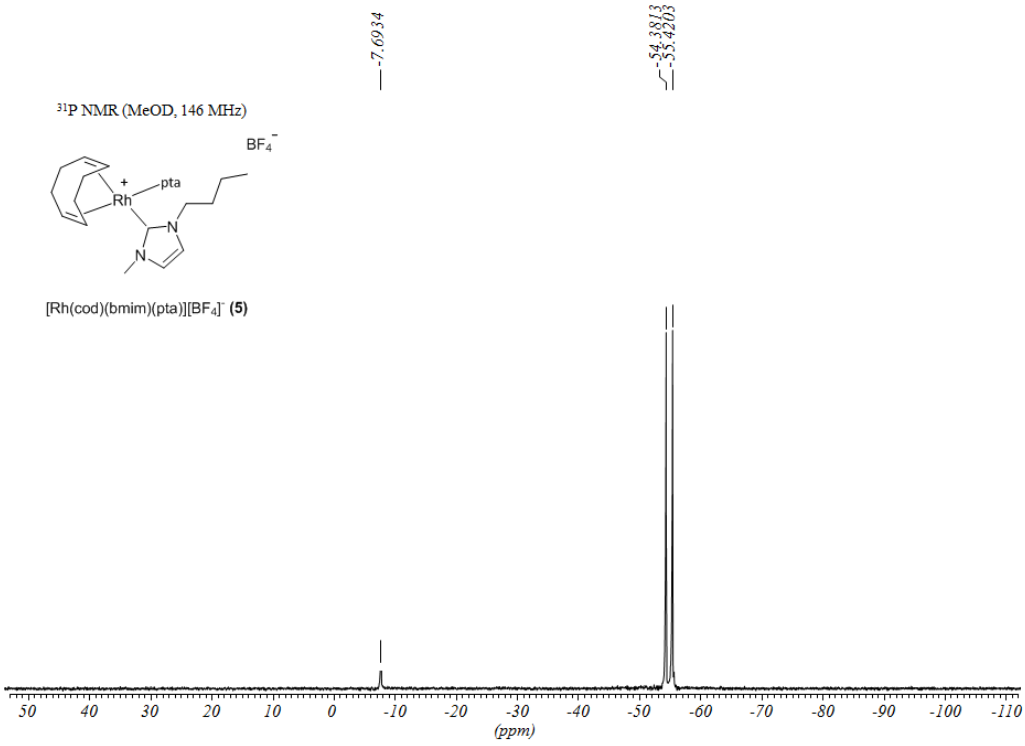

Figure S11. $^{31}P\{^{1}H\}$ NMR spectrum of $[Rh(bmim)(cod)(pta)]BF_4$ (**5**).

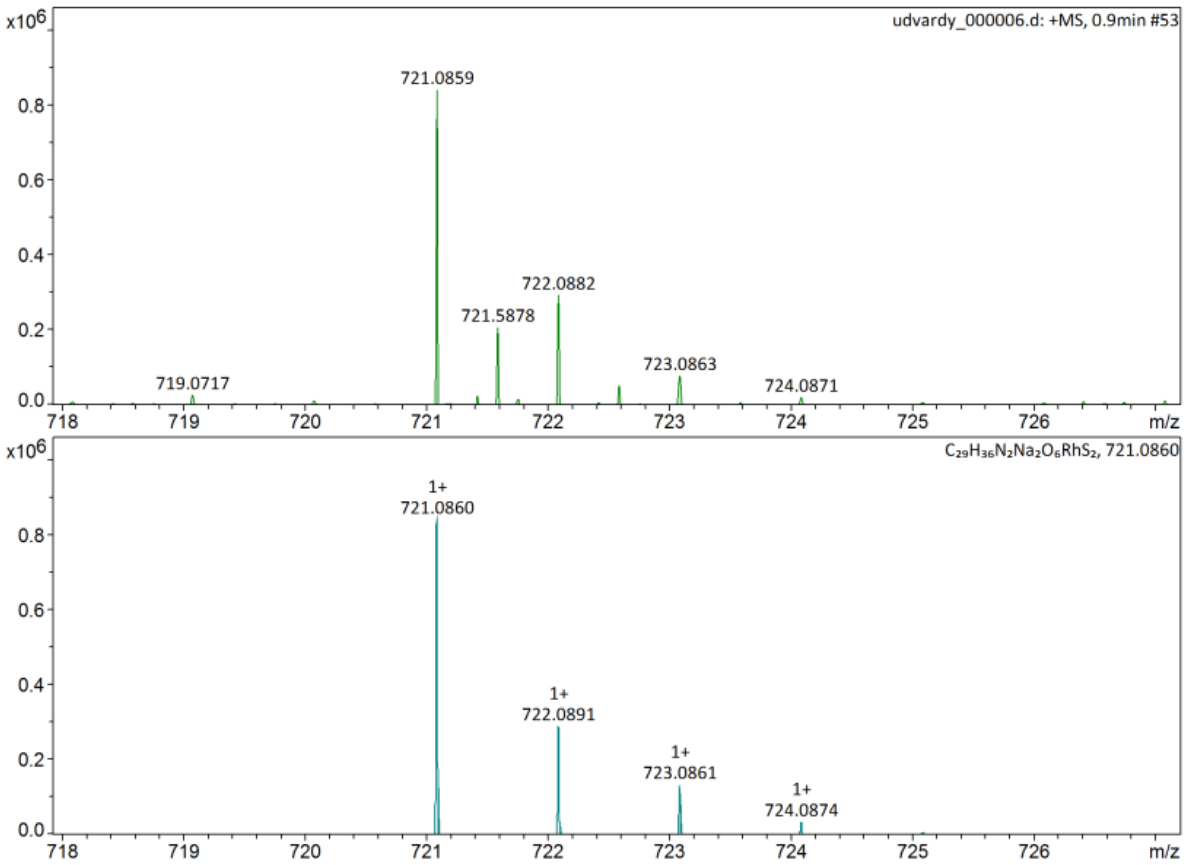

Figure S12. MS(ESI), positive mode, in MeOH, *m/z* for [RhCl(cod)(sSIMes)] (**1**) $[M\text{-}Cl]^+$ ($C_{29}H_{36}N_2Na_2O_6RhS_2$), Calculated: 721.0860, Found: 721.0859.

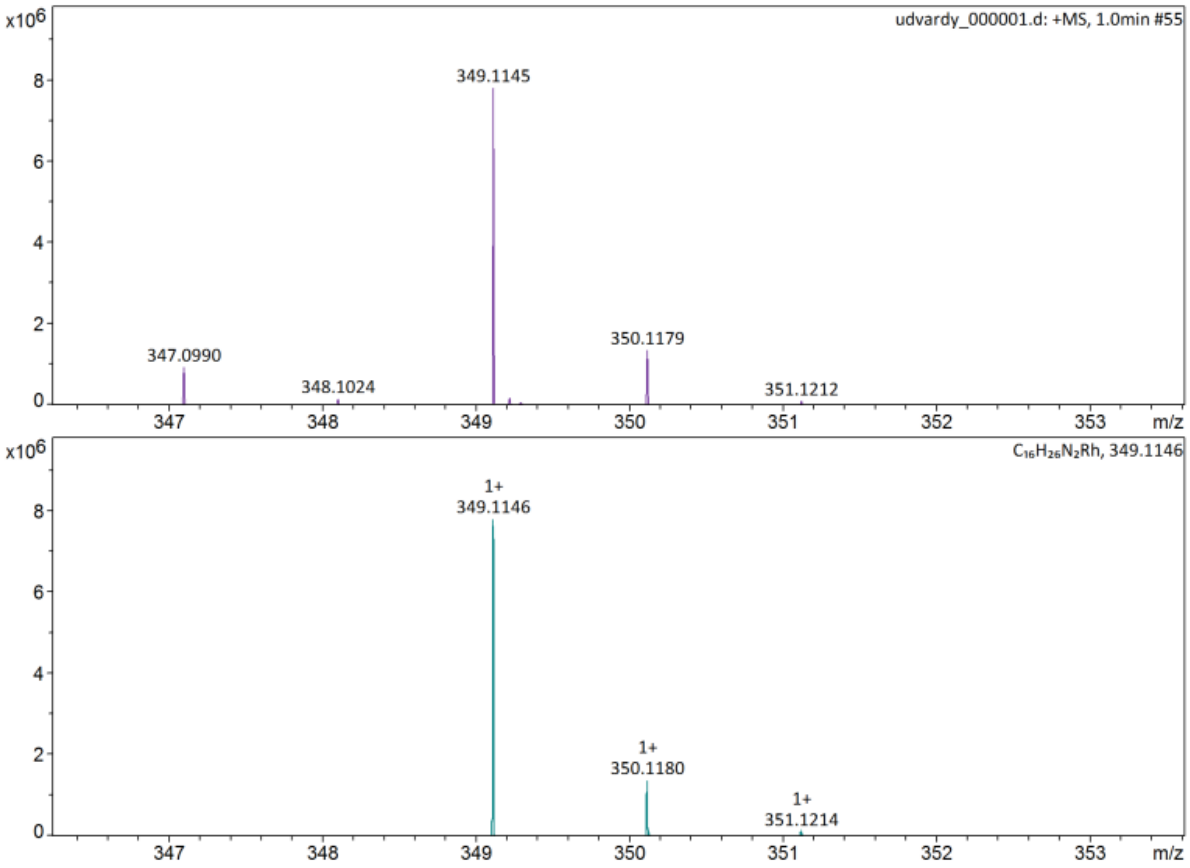

Figure S13. MS(ESI), positive mode, in MeOH, *m/z* for [RhCl(bmim)(cod)] (**3**) $[M\text{-}Cl]^+$ ($C_{22}H_{38}N_5PRh$), Calculated: 349.1146, Found: 349.1145.

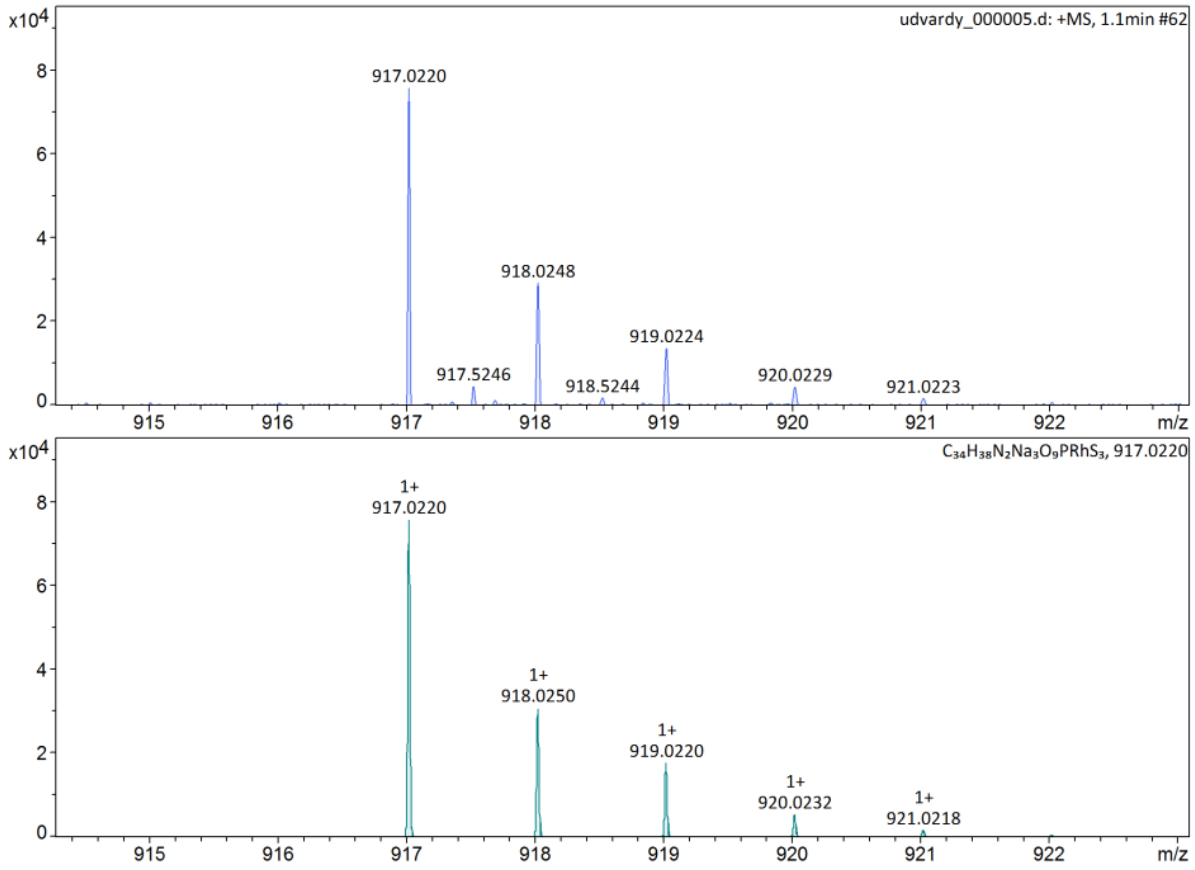

Figure S14. MS(ESI), positive mode, in MeOH, *m*/*z* for Na_2[Rh(bmim)(cod)(*m*tppts)] (**4**) $[M]^+$ ($C_{34}H_{38}N_2Na_3O_9PRhS_3$), Calculated: 917.0220, Found: 917.0220.

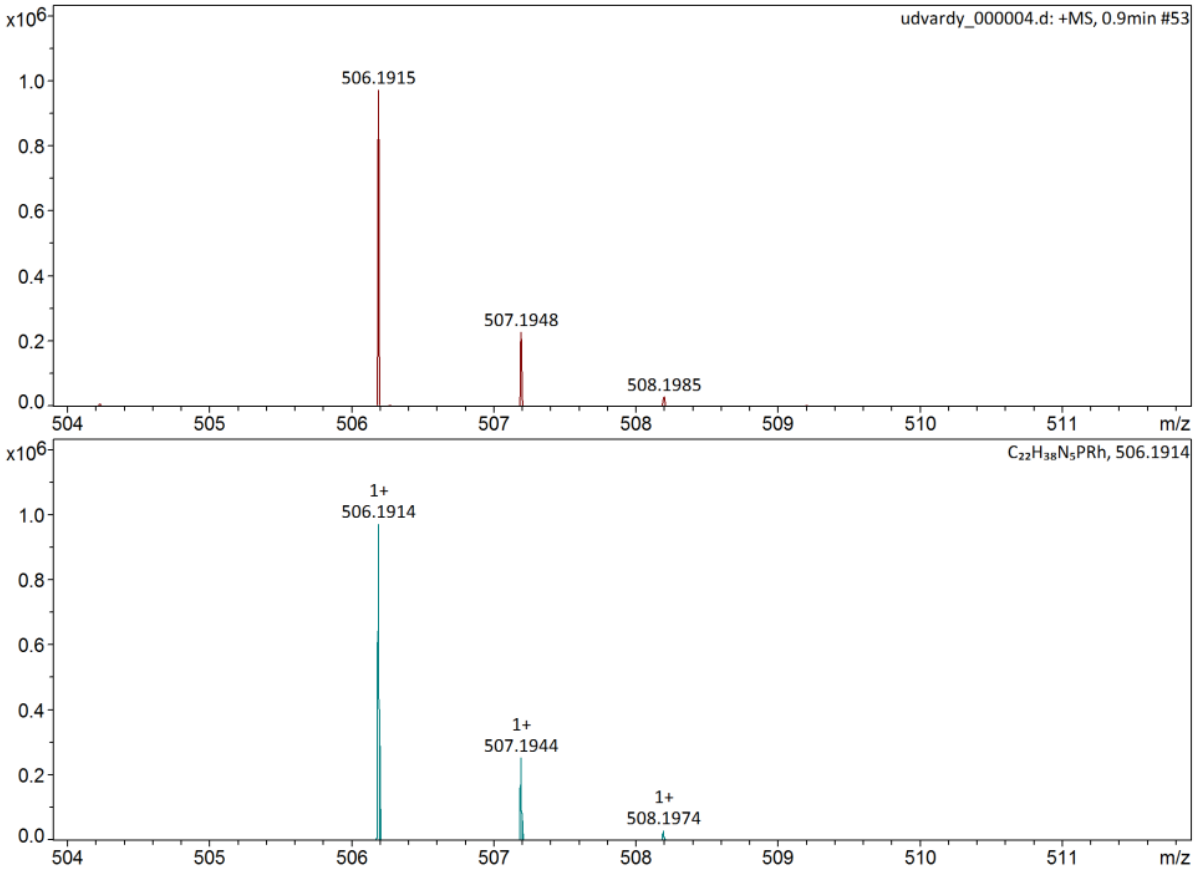

Figure S15. MS(ESI), positive mode, in MeOH, *m*/*z* for [Rh(bmim)(cod)(pta)]BF_4 (**5**) $[M\text{-}BF_4]^+$ ($C_{22}H_{38}N_5PRh$), Calculated: 506.1914, Found: 506.1915.

*Experimental details for molecular structure determination of [Rh(bmim)(cod)(pta)]BF_4 (**5**)*

A yellow block-shaped crystal with dimensions 0.51 × 0.24 × 0.10 mm^3 was mounted. Data were collected using Enraf Nonius TurboCAD4 diffractometer operating at room temperature. Data were measured using non-profiled omega/2theta scans using MoK_α radiation. The diffraction pattern was indexed and the total number of runs and images was based on the strategy calculation from the program CAD4 Express [1] The maximum resolution that was achieved was Θ = 25.606° (0.82 Å). The diffraction pattern was indexed and the total number of runs and images was based on the strategy calculation from the program CAD4 Express. The unit cell was refined using XCAD4 on 25 reflections. Data reduction, scaling and absorption corrections were performed using XCAD4 [2]. The final completeness is 98.90 % out to 25.606° in Θ. A PSI-SCAN absorption correction was performed using [3] number of PSI-SCAN sets used was 3 Theta correction was applied. Averaged transmission function was used. Fourier smoothing - Window value 5. The absorption coefficient μ of this material is 0.784 mm^{-1} at this wavelength (λ= 0.71073).

The structure was solved by the ShelXT [4] structure solution program using dual methods and refined by full matrix least squares minimisation on $\boldsymbol{F^2}$ using ShelXL [5] managed with $OLEX^2$ [6] and WINGX [7]. All non-hydrogen atoms were refined anisotropically. Most hydrogen atom positions were calculated geometrically and refined using the riding model, but some hydrogen atoms were refined freely. In the crystal lattice BF_4-ion is disordered with 32% and 68% occupancies.

Publication materials were prepared using the Mercury CSD 4.3.0 software [8], Platon [9] and ReportPlus an $Olex^2$ extension.

Table S1. Experimental details of X-ray diffraction measurement

Compound	**Complex 5**
Formula	$C_{22}H_{38}BF_4N_5PRh$
Formula Weight	593.26
Colour	yellow
Shape	block
Size/mm^3	0.10×0.24×0.51
T/K	293(2)
Crystal System	Monoclinic
Space Group	$P2_1/n$
a/Å	12.0011(16)
b/Å	11.460(6)
c/Å	18.6275(14)
$\alpha/^\circ$	90
$\beta/^\circ$	96.66(4)
$\gamma/^\circ$	90
V/Å^3	2544.6(14)
Z	4
Z'	1
Wavelength/Å	0.71073
Radiation type	MoK_α
$D_{calc.}$/ g cm^{-3}	1.549
μ/mm^{-1}	0.784
2Θ range for data collection/°	5.60 – 51.20
Reflections collected	5107
Index Range	$0 \le h \le 14$, $0 \le k \le 13$, $-22 \le l \le 22$
Independent reflections	4740 [R_{int} = 0.044]
Data/restraints/parameters	4740/10/375
GooF	1.064
wR_2 (all data)	0.1297
wR_2	0.1245
R_1 (all data)	0.0500
R_1	0.0444
Largest diff. peak/hole / e Å^{-3}	1.92/– 0.77

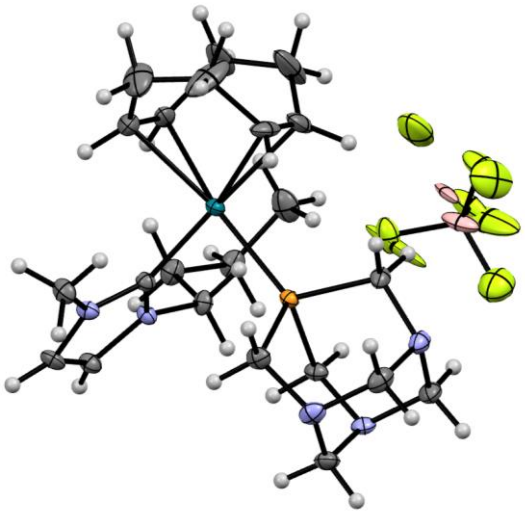

Figure S16. ORTEP view with 50% thermal ellipsoids of [Rh(bmim)(cod)(pta)]BF_4 (**5**)

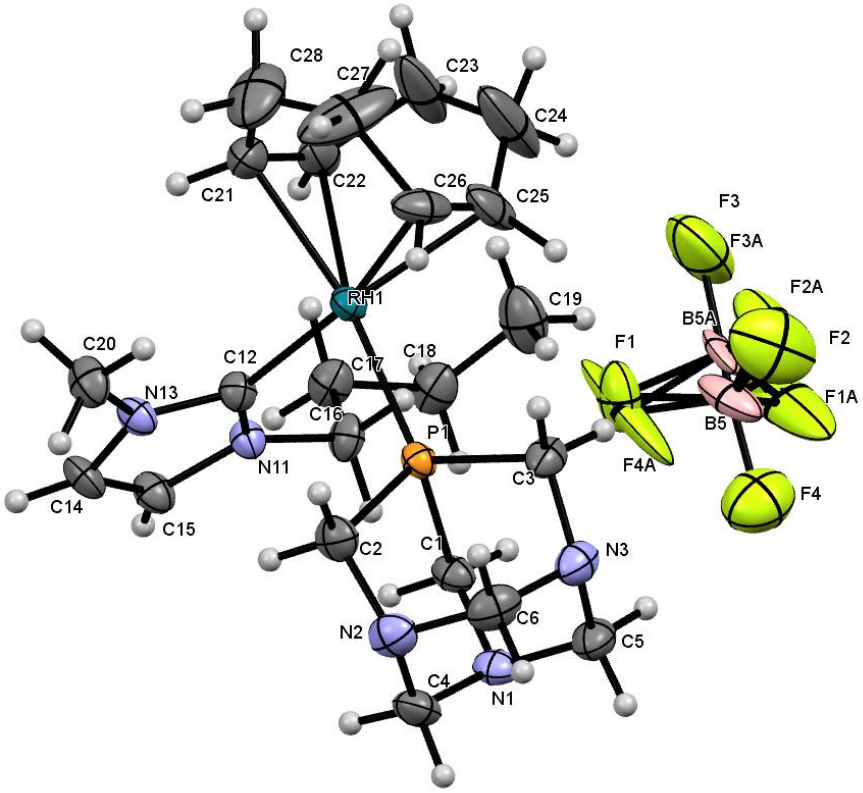

Figure S17. ORTEP diagram of [Rh(bmim)(cod)(pta)]BF_4 (**5**) at 50% probability level, showing the numbering system.

Table S2: Bond lengths for [Rh(bmim)(cod)(pta)]BF_4 (**5**)

Atom	Atom	Length/Å
C1	N1	1.467(5)
C1	P1	1.849(4)
C2	N2	1.467(6)
C2	P1	1.847(4)
C3	N3	1.462(6)
C3	P1	1.841(4)
C4	N1	1.454(6)
C4	N2	1.463(6)
C5	N1	1.468(6)
C5	N3	1.464(6)
C6	N2	1.457(6)
C6	N3	1.457(6)
C12	N11	1.356(5)
C12	N13	1.346(5)
C12	Rh1	2.025(4)
C14	C15	1.333(6)
C14	N13	1.377(5)
C15	N11	1.378(5)
C16	C17	1.510(6)
C16	N11	1.467(5)
C17	C18	1.526(6)
C18	C19	1.503(8)
C20	N13	1.452(5)
C21	C22	1.359(7)
C21	C28	1.496(8)
C21	Rh1	2.214(5)
C22	C23	1.510(7)
C22	Rh1	2.218(4)
C23	C24	1.421(8)
C24	C25	1.468(8)
C25	C26	1.356(8)
C25	Rh1	2.212(4)
C26	C27	1.497(8)
C26	Rh1	2.208(4)
C27	C28	1.412(9)
P1	Rh1	2.2668(11)

Table S3. Bond angles for [Rh(bmim)(cod)(pta)]BF_4 (**5**).

Atom	Atom	Atom	Angle/°
N1	C1	P1	112.6(3)
N2	C2	P1	112.2(3)
N3	C3	P1	112.7(3)
N1	C4	N2	114.3(3)
N1	C5	N3	114.6(4)
N3	C6	N2	115.0(4)
N11	C12	Rh1	128.5(3)
N13	C12	N11	104.3(3)
N13	C12	Rh1	127.3(3)
C15	C14	N13	106.1(4)
C14	C15	N11	107.3(4)
N11	C16	C17	112.8(3)
C16	C17	C18	110.5(4)
C19	C18	C17	113.6(4)
C22	C21	C28	127.0(5)
C22	C21	Rh1	72.3(3)
C28	C21	Rh1	108.1(4)
C21	C22	C23	124.7(5)
C21	C22	Rh1	72.3(3)
C23	C22	Rh1	109.1(3)
C24	C23	C22	118.5(5)
C23	C24	C25	118.6(5)
C24	C25	Rh1	109.5(3)
C26	C25	C24	127.1(6)
C26	C25	Rh1	71.9(3)
C25	C26	C27	124.3(6)
C25	C26	Rh1	72.4(3)
C27	C26	Rh1	108.9(4)
C28	C27	C26	119.2(5)
C27	C28	C21	118.3(5)
C1	N1	C5	111.5(3)
C4	N1	C1	111.0(3)
C4	N1	C5	107.8(3)
C2	N2	C4	111.3(3)
C6	N2	C2	111.3(4)
C6	N2	C4	108.3(4)
C3	N3	C5	110.7(3)
C6	N3	C3	111.3(4)
C6	N3	C5	108.0(4)
C12	N11	C15	110.7(3)
C12	N11	C16	124.0(3)
C15	N11	C16	125.3(3)
C12	N13	C14	111.7(3)
C12	N13	C20	124.7(3)
C14	N13	C20	123.6(3)
C1	P1	Rh1	122.25(14)
C2	P1	C1	96.92(19)
C2	P1	Rh1	117.54(15)
C3	P1	C1	97.29(19)
C3	P1	C2	98.5(2)
C3	P1	Rh1	119.32(14)
C12	Rh1	C21	91.16(17)
C12	Rh1	C22	93.48(17)
C12	Rh1	C25	164.52(19)
C12	Rh1	C26	159.4(2)
C12	Rh1	P1	88.41(12)
C21	Rh1	C25	91.39(19)
C21	Rh1	P1	161.19(14)
C22	Rh1	C21	35.39(19)
C22	Rh1	C25	79.94(18)
C22	Rh1	P1	163.37(14)
C25	Rh1	P1	94.02(13)
C26	Rh1	C21	80.60(19)
C26	Rh1	C22	90.62(19)
C26	Rh1	C25	35.8(2)
C26	Rh1	P1	93.40(13)

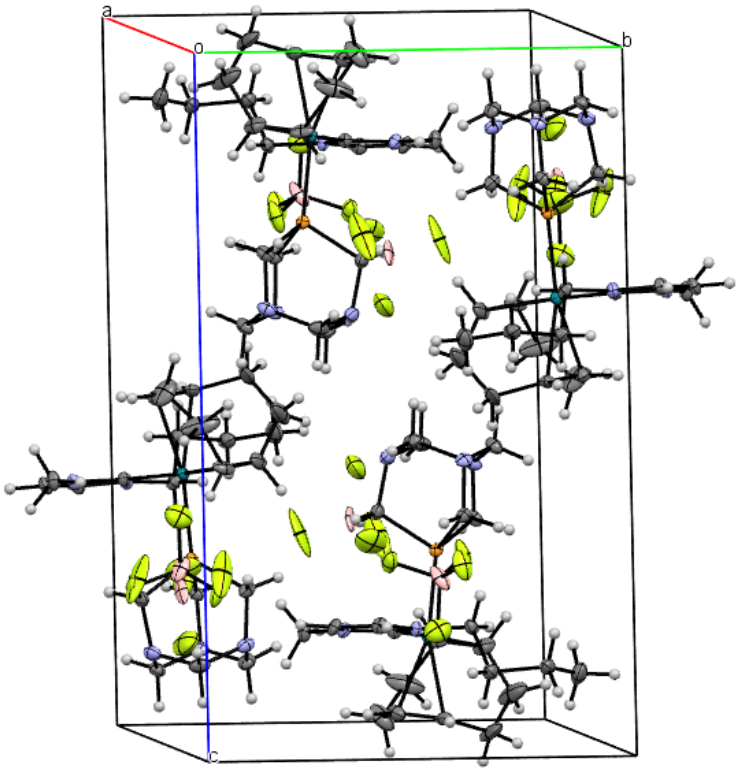

Figure S18. An ORTEP diagram of the unit cell of [Rh(bmim)(cod)(pta)]BF_4 (**5**) viewed along axis „**a**" at the 50% probability level

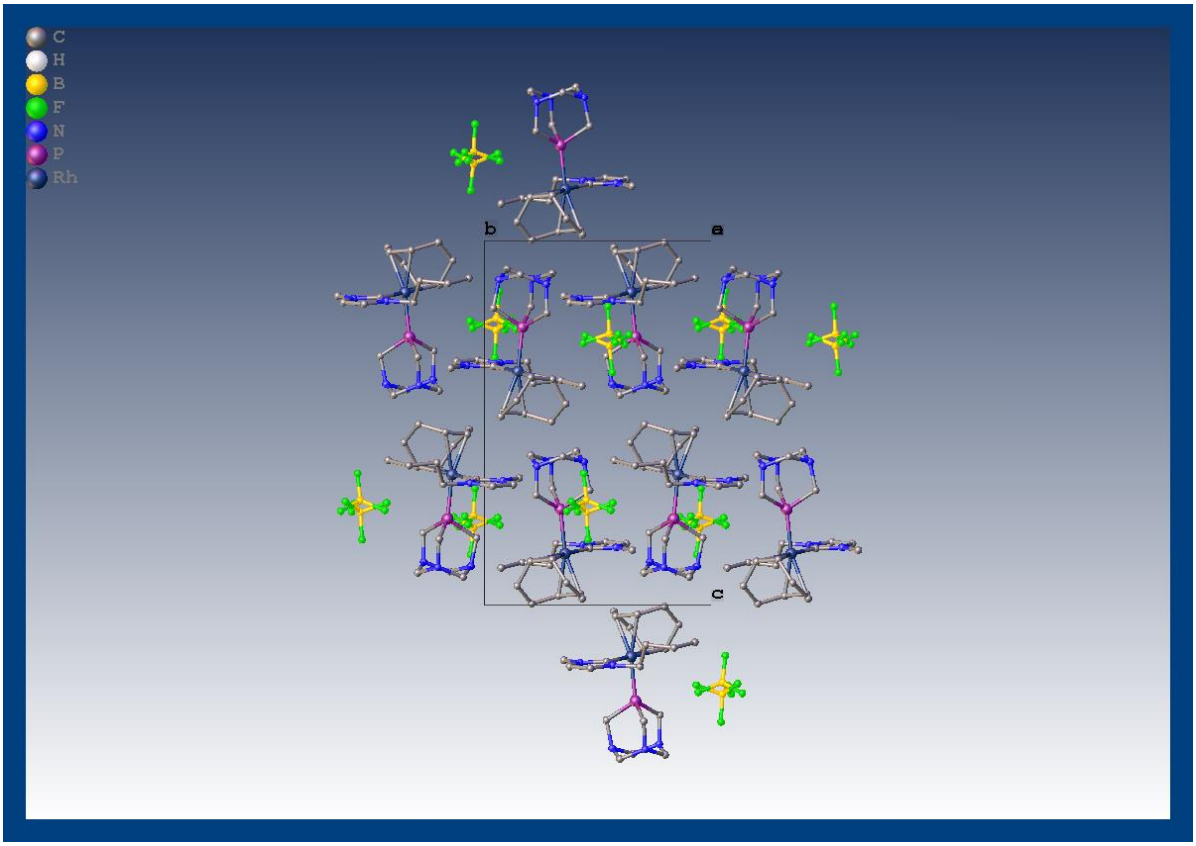

Figure S19. A packing diagram of [Rh(bmim)(cod)(pta)]BF_4 (**5**). (All hydrogen atoms have been omitted for the clarity.)

References

1. Nonius, B.V. CAD-Express Software, Ver. 5.1/1.2. Enraf Nonius, Delft, The Netherlands. **1994**.
2. Harms, K.; Wocaldo, S. XCAD4, University of Marburg, Germany. **1995**.
3. North, A.C.T.; Phillips, D.C.; Mathews, F.S. A semi-empirical method of absorption correction. *Acta Crystallographica Section A* **1968**, *24*, 351–359, doi:10.1107/S0567739468000707.
4. Sheldrick, G.M. A short history of SHELX. *Acta Cryst A* **2008**, *64*, 112–122, doi:10.1107/S0108767307043930.
5. Sheldrick, G.M. SHELXT – Integrated space-group and crystal-structure determination. *Acta Cryst A* **2015**, *71*, 3–8, doi:10.1107/S2053273314026370.
6. Dolomanov, O.V.; Bourhis, L.J.; Gildea, R.J.; Howard, J. a. K.; Puschmann, H. OLEX2: a complete structure solution, refinement and analysis program. *J Appl Cryst* **2009**, *42*, 339–341, doi:10.1107/S0021889808042726.
7. Farrugia, L.J. WinGX and ORTEP for Windows: an update. *Journal of Applied Crystallography* **2012**, *45*, 849–854, doi:10.1107/S0021889812029111.
8. Spek, A.L. checkCIF validation ALERTS: what they mean and how to respond. *Acta Crystallographica Section E* **2020**, *76*, 1–11, doi:10.1107/S2056989019016244.
9. Macrae, C.F.; Bruno, I.J.; Chisholm, J.A.; Edgington, P.R.; McCabe, P.; Pidcock, E.; Rodriguez-Monge, L.; Taylor, R.; Streek, J. van de; Wood, P.A. Mercury CSD 2.0 – new

features for the visualization and investigation of crystal structures. *J Appl Cryst* **2008**, *41*, 466–470, doi:10.1107/S0021889807067908.